Fluid-solid equilibrium of a charged hard-sphere model

Carlos Vega,[1] Fernando Bresme,[1,2] and José L.F. Abascal[1]
[1]*Departamento de Química-Física, Facultad de Ciencias Químicas, Universidad Complutense de Madrid, E-28040 Madrid, Spain*
[2] *Instituto de Química-Física Rocasolano, CSIC, Serrano 119, E-28006 Madrid, Spain*
(Received 30 April 1996)

The fluid-solid equilibrium of a system made of charged hard spheres with positive and negative ions of the same size is considered. At high temperatures freezing occurs in a substitutionally disordered close packed structure, the face centered cubic solid (fcc). At low temperatures freezing occurs in the ordered cesium chloride structure (CsCl). As the latter solid coexists with the fcc structure at high densities, two triple points exist on the phase diagram. By using computer simulation we determine the precise location of both triple points. In the first of them, vapor, liquid, and solid (CsCl) are in equilibrium at $T^* = T/[q^2/(\sigma k \epsilon)] = 0.0225$, where q is the charge of the ions, σ their diameters, k the Boltzmann constant, and ϵ the dielectric constant. In the other triple point, occurring at $T^* = 0.24$, the three coexisting phases are the fluid, a CsCl solid, and the fcc solid. The vapor-liquid-solid triple point temperature is found to be about one-third of the critical temperature, in good agreement with the experimental ratio for a number of molten salts. An implementation of the cell theory for the solid phases of charged hard spheres is presented. It is shown that this simple theory provides a reasonable description of the properties of solid charged hard spheres. When the theory is combined with an accurate theory for the fluid phase a very satisfactory description of the phase diagram of charged hard spheres is obtained. The cell theory predictions are better than those recently reported using a density functional scheme. [S1063-651X(96)05009-X]

PACS number(s): 64.70.Dv, 64.70.Hz, 64.70.Kb, 61.20.Gy

I. INTRODUCTION

The structure of molecular fluids at high densities is dominated by repulsive forces [1,2]. In the case of ionic systems the structure is determined simultaneously by the short range repulsive forces and by the strength and *asymmetry* of the Coulombic interactions. For this reason it is believed that the study of hard ionic systems is of great value for improving our understanding of real ionic substances such as molten salts. It is expected that dispersive attractive forces could be incorporated in a perturbative way once the properties of hard Coulombic systems are well known.

This paper is devoted to a charged hard-sphere model usually known as the restricted primitive model (RPM). The model has played a fundamental role in the study of ionic systems, in some sense similar to the role played by the hard-sphere model (HS) in the study of neutral systems. It consists of a mixture of hard spheres, half of them carrying positive charge and the remainder carrying negative charge. The particle diameter is taken to be the same for both species. The RPM is not realistic as it does not incorporate attractive dispersion forces and uses a too simple form for the repulsive ones. Nevertheless, it provides a fair description, as compared with the experimental values, of several salts in the molten state. The study of charged hard spheres has been performed in a number of previous studies (see Ref. [3] for an excellent review). The issues addressed in these works can be considered of three different types. The first one was centered on the determination of the structure and properties of the charged hard spheres in the fluid phase. The solution of the Ornstein-Zernike equation within the mean spherical approximation (MSA) performed by Waisman and Lebowitz [4,5] in the 1970s, and the computer simulations performed by several groups [6–8] played a fundamental role. It was soon clear that there was room to improve the thermodynamic predictions of the MSA theory and a little bit later Larsen *et al.* [9] proposed an improved version, the so-called Truncated $\Gamma 2$ approximation (TΓ2A), which yields reasonable predictions for the thermodynamic properties of charged hard spheres at medium and high densities. The second area of study was the computation of the vapor-liquid equilibrium of the restricted primitive model. Vorontsov-Vel'yaminov and Chasovskikh by using Monte Carlo computer simulations showed the existence of a gas-liquid coexistence [10,11]. Stell *et al.* [12] also predicted the existence of this vapor-liquid equilibrium, by using several theoretical approaches. Recent computer simulations carried out by several groups [13–17] have definitively established the existence of the vapor–liquid equilibrium for the restricted primitive model. In spite of the great deal of work concerning this Hamiltonian there are some problems that are not yet solved and are the focus of current work. Two examples of that are the theoretical treatment of the gas phase [18–21] and the explanation of the apparent classical character of the critical exponents in ionic fluids [22,23].

This paper concerns a third issue in the study of the RPM, the fluid-solid transition. Unlike the first and second areas referred to above, comparatively this one has received much less attention. This is in contrast with other models more or less related with ionic systems, such as the classical one component plasma (OCP) or the Yukawa models for which the fluid-solid equilibrium is well known [24–29]. Nevertheless, as early as 1968, Stillinger and Lovett [30] sketched the phase diagram of charged hard spheres including the fluid-solid transition. Twenty years later, Barrat [31] used the density functional theory in the description of the freezing of charged hard spheres. Recently Smit *et al.* [32] employed Monte Carlo computer simulations in order to determine the

fluid-solid equilibrium of this model. The works by Barrat and Smit *et al.* investigated two stable solid phases. At low temperatures, the stable structure of the solid is that commonly denoted as cesium chloride whereas at high temperatures the stable solid is that obtained from the close packing structure of hard spheres with a random allocation of cations and anions arranged in a face centered cubic lattice. Therefore these recent studies would confirm the picture by Stillinger and Lovett almost 30 years ago [30].

In spite of this recent and important progress concerning the fluid-solid equilibrium of the RPM the situation is not quite satisfactory. Firstly, the triple point of charged hard spheres has not been precisely determined. A tentative estimation is now available [32], namely, $T^*=T/[q^2/(\sigma k\epsilon)]=0.025$, where T is the temperature, q the ionic charge, σ the ionic diameter, k the Boltzmann constant, and ϵ the dielectric constant. This estimate was obtained by extrapolating to low temperatures the Monte Carlo coexistence points at high temperatures. On the other hand, the theoretical treatment of the fluid-solid transition of the RPM reduces to the work by Barrat [31]. Although the density functional theory has played an important role in improving our understanding of the fluid-solid equilibrium of a number of simple systems [36–39], this first theoretical attempt to describe the fluid-solid equilibrium of the RPM does not yield quantitative agreement with simulation so that there is room for theoretical improvement.

The aim of this paper is twofold. Firstly, we intend to extend the previous Monte Carlo computations by Smit *et al.* [32] in order to obtain a precise estimation of the triple points. In addition we introduce a slight modification of the cell theory of Lennard-Jones and Devonshire [33,34], and apply it to the study of the solid phases of the RPM. The theory for the solid is combined with the TΓ2A scheme for the fluid in order to compute on a purely theoretical basis the fluid-solid diagram. This strategy of combining an accurate theory for the liquid with the cell theory for the solid was pioneered by Henderson and Barker some time ago [35]. Recent work has shown the ability of the cell theory to describe fairly complicated solids such as, for instance, hard dumbbells, [40,41] quadrupolar hard dumbbells [42,43], and mixtures of hard spheres [44–46]. Therefore the possibility of using cell theory for describing complicated solids should not be overlooked. In this work it is shown that this extension is also possible for a rather complicated system as the RPM. The scheme of the paper is as follows. In Sec. II we report the implementation of the cell theory for the restricted primitive model. Details of the simulations performed in this work are described in Sec. III. Section IV presents the results and Sec. V closes with the conclusions of this paper.

II. THE CELL THEORY

The restricted primitive model is defined as an equimolar mixture of anions and cations which interact through the following potential

$$u(r)=u_{\mathrm{HS}}+u_{qq}, \tag{2.1a}$$

$$u_{\mathrm{HS}}=\begin{cases}\infty & \text{if } r<\sigma\\ 0 & \text{if } r\geqslant\sigma,\end{cases} \tag{2.1b}$$

$$u_{qq}=\pm\frac{q^2}{\epsilon r}, \tag{2.1c}$$

where u_{HS} is the hard-sphere potential, q is the ionic charge, ϵ is the dielectric constant of the medium, and σ the hard-sphere diameter taken to be the same for both species and the plus and minus signs apply, respectively, to the interaction between ions of the same and different charge. The reduced number density of the system is defined as $\rho^*=\rho\sigma^3=N\sigma^3/V$, N being the total number of ions filling a volume V. In the same way, we define the reduced temperature T^* and its inverse β^*, as $T^*=1/\beta^*=kT\epsilon\sigma/q^2$. Finally, the reduced pressure is $P^*=P\epsilon\sigma^4/q^2$.

Let us consider the RPM as a binary system. Let $N_A=N/2$ the number of cations referred to here as component A, and $N_B=N/2$ the number of anions, referred to as component B. We assume that components A and B have the same mass. We start by developing the cell theory for an ordered structure such as those of CsCl or NaCl. The unit cell of these structures is presented in Fig. 1. The CsCl lattice has a coordination number of 8, which in NaCl is 6. In these two structures the ions A and B are located in the solid within two different sublattices [cf. Figs. 1(a) and (b)]. The classical partition function for this system is given by

$$Q=\frac{(\Lambda_t)^{-3N}}{N_A!N_B!}Q', \tag{2.2a}$$

$$Q'=\int \exp[-\beta\mathcal{U}(1,2..N)]d1,\ldots,dN, \tag{2.2b}$$

where $\Lambda_t=[h^2/(2\pi mkT)]^{1/2}$, $\beta=1/kT$, and $\mathcal{U}(1,2,\ldots,N)$ is the total energy of the system. Let us define $U(\mathbf{r}_1)$ as the energy of a central ion—labeled as 1—located at $\mathbf{r}_1$ with the remainder of the ions of the solid resting at their equilibrium positions,

$$U(\mathbf{r}_1)=\sum_{j=2}^{N}[u_{\mathrm{HS}}(\mathbf{r}_1,\mathbf{r}_j)+u_{qq}(\mathbf{r}_1,\mathbf{r}_j)]. \tag{2.3}$$

Because of its definition, $U(\mathbf{r}_1)$ depends only on the position of the central ion, $\mathbf{r}_1$. Next, we split $U(\mathbf{r}_1)$ into two terms [47],

$$U(\mathbf{r}_1)=U_0+\Delta U(\mathbf{r}_1), \tag{2.4}$$

where U_0 is the lattice energy of molecule 1 when fixed on the lattice position. For charged hard spheres U_0 is just the Coulombic energy of a central ion with the rest of the ions in the crystal, all the particles located at the lattice positions. Given the symmetry of the RPM it is clear that the value of U_0 is the same for particles A and B. Actually, U_0 is related to the Madelung constant, which is a function of the lattice in consideration. In the context of the cell theory, the free energy of the solid phase A^{RPM} is given by [34,47]

$$A^{\mathrm{RPM}}=-NkT\ln\frac{v_f}{\Lambda_t^3}+N\frac{U_0}{2}. \tag{2.5}$$

The disappearance of the terms $N_A!$ and $N_B!$ in Eq. (2.5) may appear surprising. This is due to the fact that there are $N_A!$

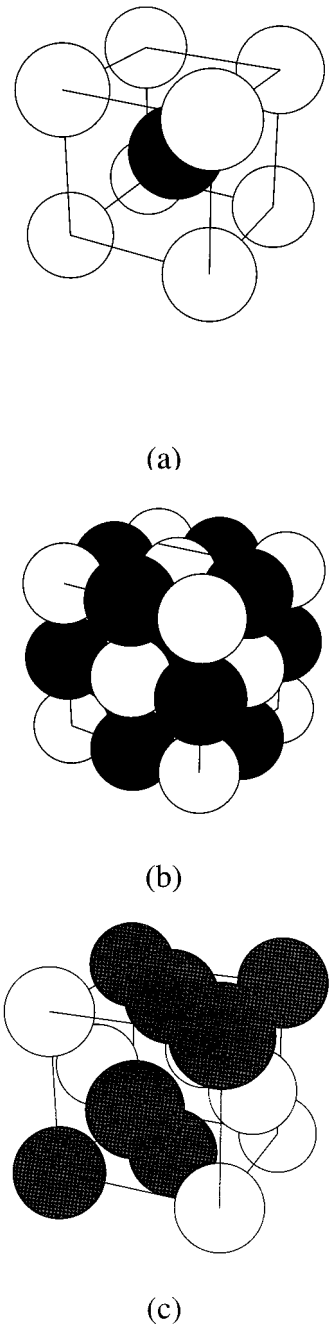

FIG. 1. Different types of possible solid structures for the RPM model. (a) CsCl structure. (b) NaCl structure. (c) fcc structure.

arbitrary ways of locating the A particles within the A sublattice, and $N_B!$ arbitrary ways of locating the particles B within the B sublattice. The free volume v_f is defined as

$$v_f = \int \exp[-\beta \Delta U(\mathbf{r}_1)] d\mathbf{r}_1 . \tag{2.6}$$

Recall that, in evaluating v_f using Eq. (2.6), all the ions of the solid stay at their equilibrium positions, and only the central ion (labeled 1) is allowed to wander within its cage. The Λ_t term in Eq. (2.5) acts as a constant present in the fluid and solid phases and therefore we may set it to an arbitrary value, namely, σ. The free energy of the solid can then be written as

$$\frac{A^{\mathrm{RPM}}}{NkT} = \frac{U_0}{2kT} - \ln \frac{v_f}{\sigma^3}. \tag{2.7}$$

According to Eq. (2.7) the free energy of the solid may be computed provided that U_0 and $\Delta U(\mathbf{r}_1)$ are known quantities. The electrostatic energy U_0 of the RPM solid can be easily evaluated from the Madelung constant M through the relation

$$U_0 = \frac{-Mq^2}{\epsilon R}, \tag{2.8}$$

where R is the nearest neighbor distance between ions. Values of the Madelung constant for the cesium chloride (CsCl) and the sodium chloride (NaCl) structures are $M = 1.76267$ and $M = 1.74756$, respectively [48]. Values of the Madelung constant for other different lattices may also be found in Ref. [48]. Let us now focus on the evaluation of the free volume v_f. According to Eq. (2.4) the function $\Delta U(\mathbf{r}_1)$ may be written as

$$\Delta U(\mathbf{r}_1) = \sum_{j=2}^{N} [u_{\mathrm{HS}}(\mathbf{r}_1, \mathbf{r}_j) + u_{qq}(\mathbf{r}_1, \mathbf{r}_j)] - U_0 . \tag{2.9}$$

$\Delta U(\mathbf{r}_1)$ represents the difference in energy between a configuration where all particles stay at their lattice position except ion 1, which is located at $\mathbf{r}_1$, and a configuration where all particles of the system, included the central ion, stay at their lattice positions. Now, assuming that

$$\sum_{j=2}^{N} u_{qq}(\mathbf{r}_1, \mathbf{r}_j) \approx U_0 , \tag{2.10}$$

Eq. (2.9) takes the form

$$\Delta U(\mathbf{r}_1) \approx \sum_{j=2}^{N} u_{\mathrm{HS}}(\mathbf{r}_1, \mathbf{r}_j). \tag{2.11}$$

The above approximation—previously proposed by McQuarrie in a cell theory treatment of the fluid phases of ionic systems [49]—is justified if the displacements of ion 1 from the equilibrium position do not modify essentially its energy. This condition is true in a high density ionic solid where the nearest neighbors form a cage around it. The short displacements undergone by the ion 1 produce a small change of the Coulombic energy not only because the electrostatic energy is very long ranged (it decays as r^{-1}) but also because the cage implies that a separation from several neighbors leads to a similar approximation to those in the opposite direction. Recall the well known fact that the electric field at any inner point of a homogeneously charged sphere is identically zero [50] and thus the potential energy does not change when the ion moves within the sphere. Of course, the charge distribution around a central ion in the lattice is not spherical so the argument is only qualitative but it illustrates the insensitivity of the Coulombic energy to the location of the central particle. An additional advantage of using the approximation

TABLE I. Constants C, a_1,a_2, and a_3 for several solid structures. The value of the closest packing density ρ^*_{cp} is also given .

Solid	C	a_1	a_2	a_3	ρ^*_{cp}
CsCl	0.2544330	-0.6513693	0.046946764	0.08519676	$3/4\sqrt{3}$
NaCl	0.29059774	-0.49111125	-0.34758300	0.77516448	1
fcc	0.20930	-0.8627	0.30679	-0.082663	$\sqrt{2}$

given by Eq. (2.11) is that now v_f acquires a clear and simple physical meaning. It represents the volume where the central ion 1 can move without overlapping its nearest neighbors.

Buehler *et al.* [51] deduced an analytical expression for v_f for a close packed fcc structure. In this work, the calculation of the free volume for the CsCl and the NaCl structures is done numerically. The reader is referred to Ref. [40] for a detailed discussion of a similar computation. In general, it is helpful to express the free volume as a function of the density of the system. We use here the expression proposed by Alder *et al.* [52]:

$$\frac{v_f}{\sigma^3} = C\alpha^3 \exp(a_1\alpha + a_2\alpha^2 + a_3\alpha^3), \tag{2.12}$$

where α is defined as

$$\alpha = \frac{\rho^*_{cp} - \rho^*}{\rho^*}, \tag{2.13}$$

ρ^*_{cp} being the close packing reduced number density of the lattice in consideration. Close packing densities for the fcc structure, CsCl structure, and NaCl structures are $\sqrt{2}$, $(3/4)\sqrt{3}$, and 1, respectively. The data of free volume for CsCl and NaCl structures are fitted according to Eqs. (2.12) and (2.13). For computational convenience, we also fit to these functions the results obtained using the analytical expression by Buehler *et al.* [51] for the fcc structure. The coefficients resulting from these fittings are reported in Table I. Equations (2.7), (2.8), and (2.12) constitute the cell theory employed in this work for the computation of the solid phase of the RPM. Given the simplicity of the theory, free energies for the solid phase may be computed with a pocket calculator.

TABLE II. Simulation results for the fluid at $\rho^* = 0.55$.

β^*	$U/(NkT)$	$g_{++}(\sigma)$	$g_{-+}(\sigma)$	Z
0.05	−0.012	2.284	2.461	3.729
0.10	−0.026	2.189	2.439	3.657
0.25	−0.087	2.090	2.663	3.708
0.50	−0.202	1.941	2.809	3.668
1.00	−0.458	1.750	2.984	3.574
2.00	−1.039	1.415	3.478	3.472
4.00	−2.318	1.032	4.167	3.222
6.00	−3.666	0.778	4.729	2.950
8.00	−5.062	0.595	5.357	2.740
10.00	−6.486	0.472	5.911	2.514
12.50	−8.304	0.338	6.675	2.271
15.00	−10.157	0.260	7.224	1.925
17.50	−12.013	0.207	8.170	1.820
20.00	−13.876	0.155	8.648	1.445
25.00	−17.687	0.106	10.026	0.940
30.00	−21.579	0.061	11.509	0.471
35.00	−25.469	0.051	13.075	0.070
40.00	−29.454	0.029	14.694	−0.338
45.00	−33.465	0.019	16.320	−0.744
50.00	−37.533	0.016	18.086	−1.085

TABLE III. Simulation results for the fluid at $\rho^* = 0.65$.

β^*	$U/(NkT)$	$g_{++}(\sigma)$	$g_{-+}(\sigma)$	Z
0.05	−0.013	2.761	2.995	4.913
0.10	−0.029	2.727	3.022	4.904
0.25	−0.093	2.582	3.201	4.906
0.50	−0.212	2.435	3.410	4.908
1.00	−0.483	2.195	3.660	4.824
2.00	−1.083	1.869	4.140	4.729
4.00	−2.403	1.338	4.830	4.397
6.00	−3.792	1.048	5.498	4.192
8.00	−5.221	0.862	5.939	3.889
10.00	−6.678	0.697	6.440	3.632
12.50	−8.524	0.530	7.070	3.332
15.00	−10.424	0.402	7.710	3.047
17.50	−12.328	0.327	8.298	2.762
20.00	−14.252	0.232	8.806	2.401
25.00	−18.149	0.149	9.832	1.744
30.00	−22.066	0.087	10.935	1.147
35.00	−26.029	0.068	12.100	0.606
40.00	−30.030	0.048	13.145	−0.030
45.00	−33.979	0.028	14.153	−0.674
50.00	−37.970	0.018	15.237	−1.273

The RPM fcc structure is a substitutionally disordered structure; i.e., cations and anions are located at the crystal lattice positions in a more or less random manner, which depends on temperature. The coordination number for this lattice is 12. A representation of a possible configuration is given in Fig. 1(c). The application of the cell theory to this structure is clearly more difficult than in the NaCl or CsCl ones. Rigorously, one should consider all the different arrangements of ions with respect to a given one. This approach was recently used in a study of the freezing of mixtures of hard spheres [44]. However, it is not clear how to implement this approach for the RPM model. The reason is twofold. Firstly, Coulombic forces are long ranged so that fluctuations in composition for second, third, and farther nearest neighbors should be considered. Besides, it is not likely that fluctuations in composition in the first coordination layer could be described by the Bragg-Williams approximation [47]. For that reason we use a different route. We start from the free energy of the RPM solid in the fcc structure using the thermodynamic relation

$$\frac{A^{\mathrm{RPM}}_{\mathrm{fcc}}(\rho^*,\beta^*)}{NkT} = \frac{A^{\mathrm{RPM}}_{\mathrm{fcc}}(\rho^*,\beta^*=0)}{NkT} + \int_0^{\beta^*} \frac{U}{NkT}\frac{d\beta'^*}{\beta'^*}. \tag{2.14}$$

The free energy of the RPM at $\beta^* = 0$ is given by

TABLE IV. Simulation results for the fluid at $\rho^*=0.75$.

β^*	$U/(NkT)$	$g_{++}(\sigma)$	$g_{-+}(\sigma)$	Z
0.05	−0.015	3.428	3.730	6.617
0.10	−0.030	3.438	3.690	6.588
0.25	−0.099	3.157	3.939	6.540
0.50	−0.223	3.043	4.099	6.535
1.00	−0.505	2.745	4.453	6.485
2.00	−1.128	2.361	4.904	6.330
4.00	−2.468	1.837	5.639	6.049
6.00	−3.887	1.524	6.201	5.772
8.00	−5.328	1.246	6.892	5.615
10.0	−6.844	1.001	7.284	5.226
12.50	−8.739	0.780	7.973	4.962
15.00	−10.648	0.623	8.497	4.614
17.50	−12.612	0.498	9.188	4.403
20.00	−14.552	0.410	9.657	4.056
25.00	−18.545	0.262	10.826	3.527
30.00	−22.534	0.185	11.932	3.005
35.00	−26.599	0.105	13.147	2.542

$$\frac{A_{\rm fcc}^{\rm RPM}(\rho^*,\beta^*=0)}{NkT}=\frac{A_{\rm fcc}^{\rm HS}(\rho^*)}{NkT}-\ln 2, \qquad (2.15)$$

where $A_{\rm fcc}^{\rm HS}(\rho^*)$ is the free energy of the hard-sphere fcc solid at the same density. Note that Eqs. (2.14) and (2.15) are exact. The ln2 term in Eq. (2.15) arises from the entropy of mixing between cations and anions in the fcc solid when $\beta^*=0$ [53]. In order to obtain $A_{\rm fcc}^{\rm RPM}(\rho^*,\beta^*)$ we need to know the value of $A_{\rm fcc}^{\rm HS}(\rho^*)$ in Eq. (2.15) and U in the integrand of Eq. (2.14). For these, we make the following two approximations.

(i) The free energy of hard spheres in the fcc structure may be approximated from the cell theory. Therefore we have

$$\frac{A_{\rm fcc}^{\rm HS}(\rho^*)}{NkT}\simeq-\ln\frac{v_f}{\sigma^3}, \qquad (2.16)$$

where v_f/σ^3 is given by Eqs. (2.12) and (2.13) with the coefficients presented in Table I for the fcc structure. Equation (2.16) slightly underestimates the free energy of hard spheres in the solid phase [40].

TABLE V. Simulation results for the fluid at $\rho^*=0.85$.

β^*	$U/(NkT)$	$g_{++}(\sigma)$	$g_{-+}(\sigma)$	Z
0.05	−0.016	4.280	4.734	9.018
0.10	−0.032	4.358	4.753	9.099
0.25	−0.099	4.090	4.925	8.992
0.50	−0.228	3.954	5.144	9.022
1.00	−0.518	3.575	5.436	8.848
2.00	−1.151	3.138	6.017	8.765
4.00	−2.506	2.548	6.910	8.584
6.00	−3.972	2.161	7.506	8.281
8.00	−5.466	1.700	8.311	8.089
10.00	−6.964	1.616	8.715	7.874
12.50	−8.893	1.310	9.173	7.367
15.00	−10.876	0.980	9.942	7.097

(ii) In addition, we assume that the internal energy of the fcc solid at a given density and temperature may be approximated by that of a metastable liquid at the same density and temperature. In order to obtain the internal energy of this metastable liquid we use the TΓ2A theory (see Appendix A for further details).

After inserting these approximations in Eq. (2.14), the free energy of the fcc RPM solid reads

$$\frac{A_{\rm fcc}^{\rm RPM}(\rho^*,\beta^*)}{NkT}=-\ln\frac{v_f}{\sigma^3}-\ln 2+\int_0^{\beta^*}\frac{U^{\rm T\Gamma 2A}}{NkT}\frac{d\beta'^*}{\beta'^*}. \qquad (2.17)$$

Once the free energy for the solid is known, the pressure can be obtained by derivating with respect to volume. In order to obtain fluid-solid equilibrium, a theoretical description of the liquid is needed. In this work we use the TΓ2A theory to describe the fluid phase of the model. It is well known that this theory provides one of the most accurate descriptions now available for the RPM model at high densities [3]. In Appendix A, expressions for the free energy, internal energy, and compressibility factor within the TΓ2A framework are given.

III. MONTE CARLO COMPUTER SIMULATIONS

In addition to the theoretical approach presented in the preceding section we have carried out Monte Carlo (MC) simulations of the RPM. The aim of these simulations is to give a precise location of the triple points presented in the fluid-solid transitions. At the same time these data are useful as a reference in order to check the theory proposed in this work. The Monte Carlo [54] simulations have been performed in the canonical ensemble. A mixture of N ions of the same size, half positive and half negative, is placed in a cubic box with periodic boundary conditions. As customary in the work with charged systems, one is forced to consider with some care the computation of the Coulombic contribution to the potential energy. In this work, the Ewald summation method [55] —which has shown to perform well in the simulation of ionic systems at high densities and low temperatures [3]— is employed. Other methods such as the minimum image can lead to a violation of the lower bound for the energy, fixed by Onsager 50 years ago [56].

As usual in the Ewald procedure, the Coulombic potential is divided into two contributions; one of them is computed in the real space whereas the other one is evaluated in the reciprocal space. The relative importance of these contributions is controlled by a parameter γ. We have chosen a value such that only pairs whose distance is lower than half the box length have to be considered. This value is taken to be $\gamma L=5.6$, L being the length of the simulation box. In the reciprocal space we restrict the summation to vectors $\vec{h}_{\rm max}\leqslant\{\pm 5,\pm 5,\pm 5\}$, and such that the modulus of the vector be $|\vec{h}|^2\leqslant 27$. In addition, we assume that the system is surrounded by a conductor.

The fluid state simulations have used a sample size with 250 total ions. We have considered five isochores, $\rho^*=$ 0.55, 0.65, 0.75, and 0.85. At each density, the simulations start at high temperatures from a CsCl lattice, which rapidly

melts. The final configuration of the run is employed as the initial one for a state at the same density and lower temperature. Typically, 0.5×10^6 configurations are generated in the equilibration stage and the production runs last 1.5×10^6 attempted particle moves. The production phase is divided into 25 cycles of 60 000 configurations each to estimate the standard deviation of the internal energy. The maximum particle displacement is set between 0.04σ and 0.15σ depending on the density and temperature of the system. The acceptance rate oscillates in these conditions between 35% and 50%. The results for the four considered isochores in the fluid phase are presented in Tables II-V. The data of internal energy from these simulations have been fitted to the empirical expression proposed by Larsen [7],

$$-\frac{U}{NkT}=\beta^{*3/2}\left[\frac{u_1+u_2\beta^{*1/2}+u_3\beta^*}{u_4+\beta^{*3/2}}\right], \tag{3.1}$$

by a nonlinear least square method. The values for the coefficients are compiled in Table VI. By integrating this expression along an isochore we obtain the relationship for the free energy, which takes the form [7]

$$\begin{aligned}\frac{\delta A^{\rm RPM}_{\rm fluid}}{NkT}&=\frac{A^{\rm RPM}_{\rm fluid}(\rho^*,\beta^*)}{NkT}-\frac{A^{\rm RPM}_{\rm fluid}(\rho^*,\beta^*=0)}{NkT}\\&=\frac{2}{3}u_1\ln\left(\frac{u_4}{u_4+\beta^{*3/2}}\right)-2u_2\beta^{*1/2}-u_3\beta^*+\frac{e}{3}(u_2-u_3e)\ln\left[\frac{(e+\beta^{*1/2})^2}{e^2-e\beta^{*1/2}+\beta^*}\right]\\&\quad+\frac{2\sqrt{3}}{3}e(u_2+u_3e)\left[\arctan\left(\frac{2\beta^{*1/2}-e}{\sqrt{3}e}\right)+\frac{\pi}{6}\right],\end{aligned} \tag{3.2}$$

where $e=u_4^{1/3}$. Additionally, $A^{\rm RPM}_{\rm fluid}(\rho^*,\beta^*=0)$ is the free energy of the RPM at $\beta^*=0$, which can be related to the free energy of the hard-sphere fluid by an expression analogous to Eq. (2.15). Aside from the simulations along the isochores mentioned above, we have performed additional simulations along three isotherms in order to compute the orthobaric line. Results from these simulations are compiled in Table VII.

The compressibility factor $Z=P/(\rho kT)$ has been computed by using the virial theorem

$$Z=1+\frac{U}{3NkT}+\frac{\pi\rho^*}{3}[g_{++}(\sigma)+g_{-+}(\sigma)], \tag{3.3}$$

where $g_{++}(\sigma)$ and $g_{-+}(\sigma)$ are the contact values of the radial distribution function between ions of the same and different sign, respectively. These values are obtained through an extrapolation of the data obtained near σ. We use typically three of these points —using a histogram bin width set to 0.01σ— which have been fitted to a second degree polynomial and then extrapolated to the contact value.

We have also performed several simulations in the solid state for two different structures, a CsCl lattice and a face centered cubic one. The total number of ions was set to $N=250$ for the former and $N=256$ for the later. The NaCl structure was not considered since, as will be shown later, it is not a stable phase for the RPM. The fcc solid being a substitutionally disordered structure, one has to cope with this feature in the Monte Carlo simulations. In addition to the particle displacements, the exchange of identities between them is also attempted. These movements are important for correctly sampling the configurational space of the fcc solid. For the solid phase simulations, we have used 2×10^6 con-

TABLE VI. Values of the coefficients u_1-u_4 of Eq. (3.1) for fitting the internal energies of the fluid state isochores presented in Tables II–V.

ρ^*	u_1	u_2	u_3	u_4
0.55	2.9817 569	−1.4571 663	0.90618 474	4.6243 126
0.65	0.7420 969	−0.7945 698	0.85881 121	0.6524 566
0.75	0.5760 094	−0.7351 154	0.86771 325	0.3972 978
0.85	0.7236 594	−0.7813 350	0.88525 077	0.5926 236

TABLE VII. Simulation results for isotherms $T^*=0.03, 0.0275$ and 0.0225.

ρ^*	β^*	$U/(NkT)$	$g_{++}(\sigma)$	$g_{-+}(\sigma)$	Z
0.700	33.33	−24.977	0.099	12.091	1.610
0.675	33.33	−24.855	0.082	12.057	1.296
0.650	33.33	−24.686	0.066	11.922	0.931
0.625	33.33	−24.579	0.059	12.079	0.751
0.600	33.33	−24.404	0.058	12.062	0.481
0.575	33.33	−24.281	0.057	12.261	0.323
0.550	33.33	−24.151	0.047	12.354	0.092
0.525	33.33	−24.022	0.030	12.455	−0.143
0.500	33.33	−23.905	0.040	12.850	−0.219
0.700	36.36	−27.370	0.080	12.798	1.317
0.675	36.36	−27.246	0.071	12.892	1.081
0.650	36.36	−27.145	0.056	12.984	0.827
0.625	36.36	−26.943	0.059	12.810	0.441
0.600	36.36	−26.820	0.047	12.918	0.206
0.575	36.36	−26.672	0.045	12.931	−0.077
0.700	44.44	−33.929	0.039	14.427	0.294
0.680	44.44	−33.744	0.040	14.424	0.052
0.660	44.44	−33.626	0.030	14.149	−0.409

TABLE VIII. Simulation results for the CsCl and fcc solid structures of the RPM model.

Solid	β^*	ρ^*	$U/(NkT)$	$g_{++}(\sigma)$	$g_{-+}(\sigma)$	Z
CsCl	4.00	1.050	−3.155	0.944	10.489	0.924
CsCl	4.00	1.000	−3.097	0.847	9.020	0.869
CsCl	4.00	0.950	−3.028	0.879	7.756	0.896
CsCl	5.00	1.050	−3.959	0.800	10.668	0.791
CsCl	5.00	1.000	−3.883	0.782	8.988	0.776
CsCl	5.00	0.950	−3.807	0.758	7.889	0.764
CsCl	6.67	0.950	−5.105	0.616	7.965	0.608
CsCl	6.67	1.000	−5.211	0.594	9.125	0.585
CsCl	6.67	1.050	−5.303	0.618	10.830	0.616
CsCl	7.69	0.900	−5.792	0.546	7.120	0.560
CsCl	7.69	0.950	−5.912	0.544	7.988	0.555
CsCl	7.69	1.000	−6.028	0.494	9.160	0.527
CsCl	7.69	1.050	−6.135	0.537	10.876	0.544
CsCl	10.00	1.000	−7.872	0.402	9.264	0.386
CsCl	15.00	1.000	−11.894	0.237	9.422	0.225
CsCl	20.00	1.000	−15.939	0.125	9.493	0.118
CsCl	25.00	1.100	−20.623	0.037	13.886	10.163
CsCl	25.00	1.050	−20.304	0.057	11.162	6.568
CsCl	25.00	1.000	−19.988	0.072	9.576	4.440
CsCl	25.00	0.950	−19.679	0.089	8.462	2.948
CsCl	25.00	0.900	−19.383	0.093	7.951	2.121
CsCl	25.00	0.850	−19.100	0.108	7.771	1.647
CsCl	25.00	0.800	−18.830	0.112	7.673	1.246
CsCl	30.00	1.000	−24.042	0.051	9.697	3.194
CsCl	35.00	1.000	−28.104	0.029	9.866	1.993
CsCl	40.00	1.100	−33.145	0.005	13.933	6.007
CsCl	40.00	1.050	−32.646	0.017	11.409	2.681
CsCl	40.00	1.000	−32.172	0.020	9.973	0.741
CsCl	40.00	0.950	−31.716	0.033	9.288	-0.300
CsCl	40.00	0.900	−31.294	0.035	8.991	-0.925
CsCl	40.00	0.850	−30.941	0.042	9.276	-1.019
CsCl	40.00	0.800	−30.732	0.046	10.341	-0.542
fcc	0.05	1.10	−0.015	5.234	5.534	13.399
fcc	0.10	1.10	−0.035	5.037	5.538	13.170
fcc	0.25	1.10	−0.107	4.953	5.831	13.387
fcc	0.50	1.10	−0.246	4.729	6.003	13.280
fcc	1.00	1.10	−0.553	4.404	6.260	13.100
fcc	2.00	1.05	−1.205	3.558	6.109	11.227
fcc	2.00	1.10	−1.221	4.053	6.726	13.010
fcc	2.00	1.15	−1.237	4.824	7.760	15.742
fcc	2.00	1.20	−1.253	5.864	9.150	19.450
fcc	4.00	1.05	−2.622	3.125	6.625	10.847
fcc	4.00	1.10	−2.660	3.611	7.186	12.550
fcc	6.00	1.10	−4.409	3.322	7.298	11.764
fcc	8.00	1.10	−5.972	3.258	7.384	11.269

figurations in the equilibration and 5×10^6 for obtaining running averages. The simulation results for both the CsCl and the fcc solids are collected in Table VIII.

IV. RESULTS AND DISCUSSION

In this section we present the results obtained with the cell theory and the simulations of the RPM. Firstly, we make a comparison between theory and simulation for the solid phases of the RPM. Next, the simulation results for the fluid phase are compared with the theoretical predictions of the TΓ2A theory. This is interesting because the densities and temperatures investigated in this work cover a range not previously studied. Finally, we analyze the question of the RPM phase diagram obtained theoretically and compare it with the simulation results.

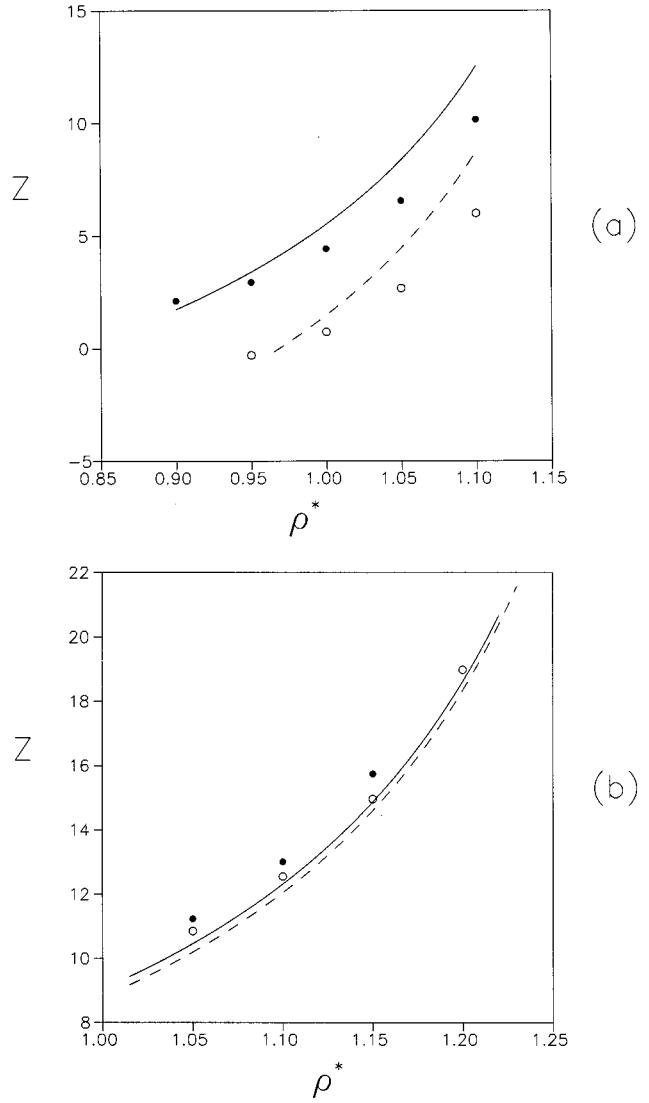

FIG. 2. Equation of state for the RPM in the solid phase as obtained from simulation (circles) and from the cell theory (lines). (a) Results for the CsCl structure for $\beta^*=25$ (solid line and filled circles) and for $\beta^*=40$ (dashed line and open circles). (b) Results for the fcc structure for $\beta^*=2$ (solid line and filled circles) and for $\beta^*=4$ (dashed line and open circles).

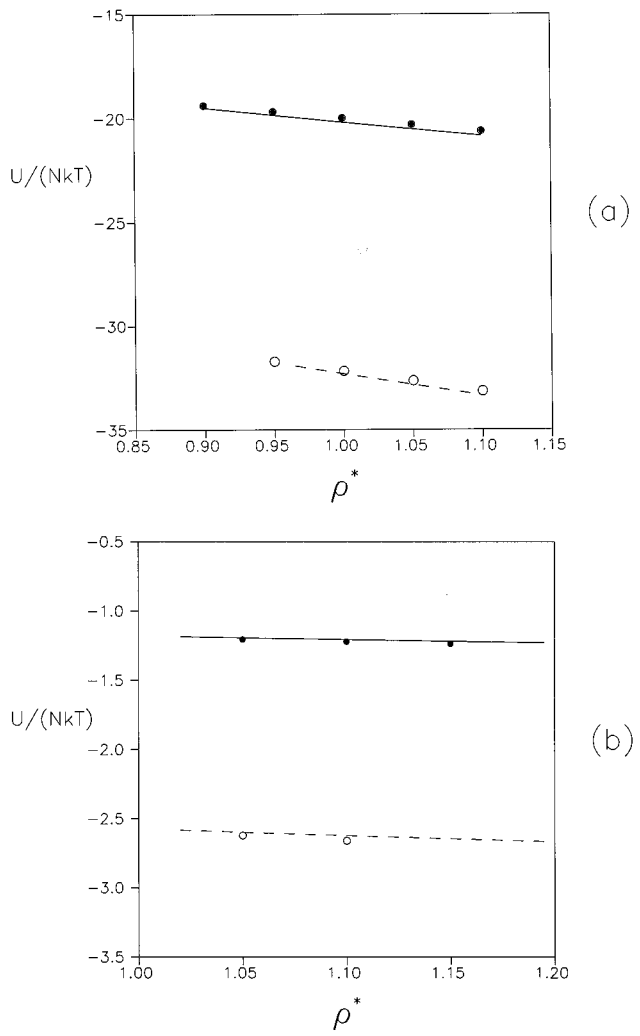

FIG. 3. Internal energy of the RPM model in the solid phase as obtained from simulation (circles) and from the cell theory (lines). (a) Results for the CsCl structure for $\beta^*=25$ (solid line and filled circles) and for $\beta^*=40$ (dashed line and open circles). (b) Results for the fcc structure for $\beta^*=2$ (solid line and filled circles) and $\beta^*=4$ (dashed line and open circles).

A. The solid state

Figure 2 shows the results for the equation of state (EOS) of the CsCl and fcc structures as obtained in our Monte Carlo simulations and using the theory presented in Sec. II. It is clear that the theory provides a fair description of the EOS of these solid phases. For the CsCl lattice [cf. Fig. 2(a)], the agreement between simulation and theory seems to be better at the lower densities where a crossing between theory and simulation is observed. This feature seems to be independent of temperature, at least for the range studied here. In the case of the fcc solid, the theory slightly underestimates the pressure. The results for the internal energy are depicted in Fig. 3. Now the theoretical predictions are in excellent agreement with the simulated values irrespective of the lattice considered. The good agreement obtained for the CsCl lattice is not surprising since the fluctuations of the ions around their lattice positions scarcely affect the internal energy, which is essentially given by the Madelung constant. For the fcc structure, the good agreement is more striking. It should be recalled that, for the fcc solid, the theoretical internal energy is that of a metastable liquid described by the TΓ2A theory. The results presented in Fig. 3(b) indicate that this seems to be a very good approximation suggesting that the substitutional disorder in the fcc solid resembles that found in the liquid.

Table IX presents the results for the free energy of the CsCl and fcc solids. Simulation results for the free energies of the CsCl structure are taken from the work by Smit *et al.* [32] whereas those for the fcc lattice are from this work. The theoretical predictions at low temperatures for the CsCl lattice compare well with the MC data. The agreement deteriorates as the temperature increases. For instance, at $T^*=0.25$ the theory overestimates the free energy by about 0.4 in NkT units. For the fcc solid, the agreement between theory and simulation is excellent. In this case, the relative error is less than 3% at the conditions studied.

TABLE IX. Free energies for the CsCl and fcc structures of the solid RPM as obtained from the simulation results of Smit *et al.* [32] for the CsCl structure and from our simulations for the fcc solid. Numbers in parentheses correspond to the free energy calculated using the cell theory of this work.

Structure	T^*	$\rho^*=1.0$	$\rho^*=1.1$	$\rho^*=1.2$
CsCl	0.04	−15.04(−15.01)	−14.40(−14.23)	
CsCl	0.05	−11.05(−10.98)	−10.29(−10.06)	
CsCl	0.10	−3.09(−2.90)		
CsCl	0.25	1.56(1.95)		
CsCl	0.50	3.11(3.56)	4.40(4.95)	
fcc	0.25		2.60(2.55)	
fcc	0.50		3.89(3.82)	5.28(5.12)
fcc	1.00		4.49(4.40)	

B. The liquid state

Next we compare our simulation results for the fluid state with the predictions of the truncated Γ2A approximation. We restrict ourselves here to the high density region we are interested in, i.e., the range $0.55<\rho^*<0.85$. Comparison at lower densities and even in the gas phase region has been reported by other authors [3,16]. From these studies it is clear that the TΓ2A theory does not perform very well at low densities. Unlike the predictions at low densities, the TΓ2A theory is quite accurate within the fluid density range considered in this work. This can be seen in Fig. 4 where we compare the predictions of the TΓ2A theory with the simulations of this work [see Eqs. (3.1) and (3.2)]. Figure 4(a) shows the free energy difference, δA, between the RPM at β^* and at $\beta^*=0$ at constant density. The agreement is very satisfactory. The compressibility factors are shown in Fig. 4(b). At the highest density studied $\rho^*=0.85$, the results of the TΓ2A theory are in excellent agreement with simulation and the theory provides a quite reliable description of the fluid. At intermediate densities, $\rho^*=0.55,0.65,0.75$, certain discrepancies between theory and simulation (especially at low temperatures) are found. We have fitted the differences between MC and the theoretical results for the isochores $\rho^*=0.55,0.65,0.75$ to the empirical expressions

$$\frac{\Delta A}{MkT}=\frac{A^{\mathrm{MC}}}{NkT}-\frac{A^{\mathrm{T}\Gamma 2\mathrm{A}}}{NkT}=(0.057019-0.168377\rho^*+0.108416\rho^{*2})\beta^*, \tag{4.1}$$

$$\Delta Z=Z^{\mathrm{MC}}-Z^{\mathrm{T}\Gamma 2\mathrm{A}}=(2.01438-8.49182\rho^*+11.6053\rho^{*2}-5.19225\rho^{*3})\beta^*. \tag{4.2}$$

By using Eqs. (4.1) and (4.2), it is possible to get results close to MC from the theory just by adding to the latter the aforementioned deviation. The fitting equations must not be used outside the density range $(0.55<\rho^*<0.75)$. For densities $\rho^*\geqslant 0.85$, the TΓ2A theory yields a very good description of the fluid phase so there is no need to include a correction term.

C. The phase diagram

In order to compute the phase diagram we need the equation of state as well as the chemical potential of all possible

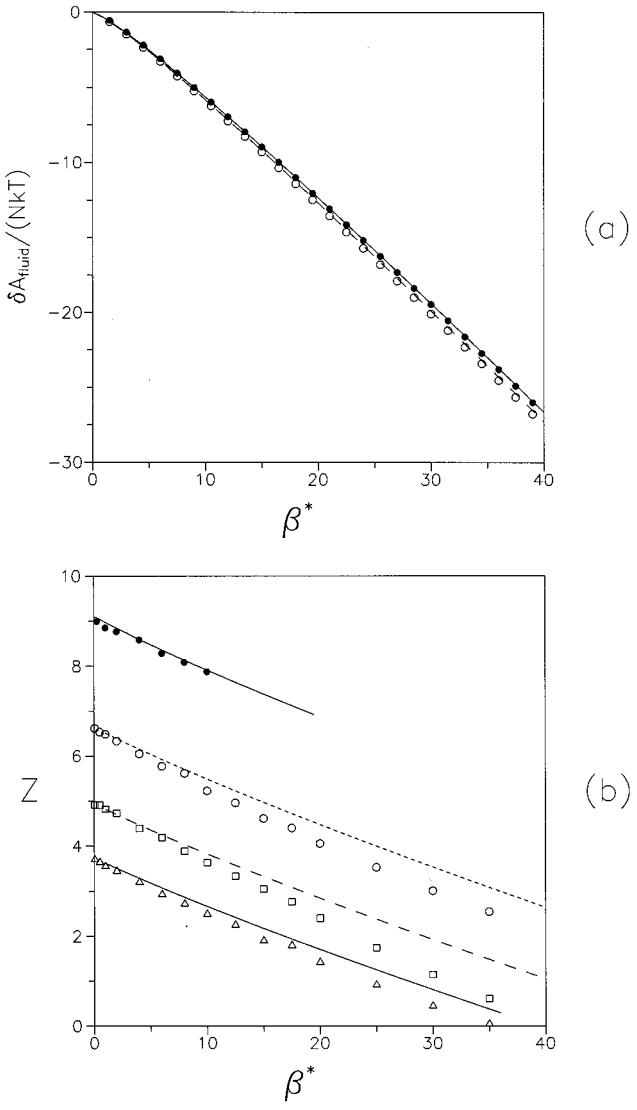

FIG. 4. Comparison between MC results (symbols) and the theoretical predictions of the TΓ2A (lines) for several isochores. (a) Free energy difference between β^* and $\beta^*=0$, $\delta A/(NkT)$, for the isochores $\rho^*=0.55$ (solid line and filled circles), and $\rho^*=0.65$ (dashed line and open circles). (b) Compressibility factor, Z, for the isochores $\rho^*=0.55$ (bottom solid line and triangles), 0.65 (dashed line and squares), 0.75 (short dashed line and circles), and 0.85 (upper solid line and filled circles).

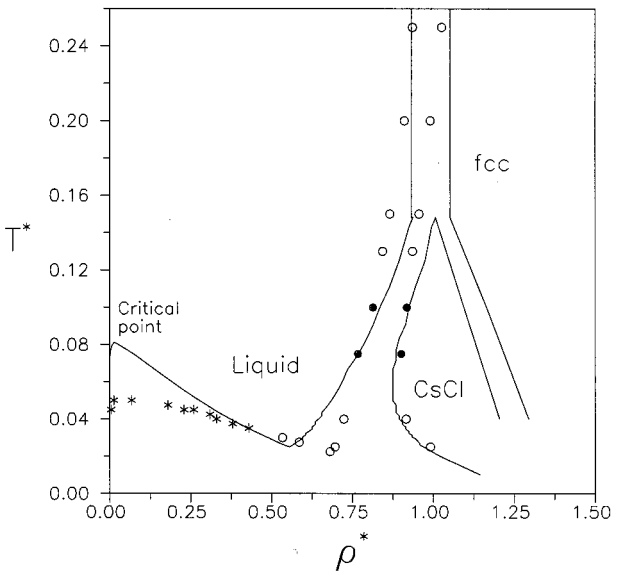

FIG. 5. Phase diagram of the RPM as computed from the theory of this work (solid lines) and from computer simulation (symbols). The vapor-liquid equilibrium data (asterisks) were taken from the Gibbs ensemble simulations of Orkoulas and Panagiotopoulos [14]. Orthobaric densities at low temperatures correspond to zero pressure densities as obtained from the simulations of this work. The fluid-solid (CsCl) data for $T^*=0.075$ and $T^*=0.10$ (filled circles) have been taken from the simulation results of Smit *et al.* [32]. The remaining symbols correspond to the fluid-solid (CsCl) equilibrium as obtained from the computer simulations of this work except for the highest temperature, which corresponds to the fluid-solid (fcc) equilibrium.

phases. Coexistence between two phases occurs when the chemical potential and pressure is the same for both phases at a given temperature. This condition can be trivially implemented for the theoretical results but the discrete nature of the simulation data forces us to make interpolations. The interpolating procedure to calculate the coexistence lines and the triple points are described in Appendix B. Figure 5 displays what can be considered the main result of this work, namely, the phase diagram of the RPM as obtained from the theory and from simulation. Let us first discuss the results for the vapor-liquid equilibrium. It is well known that the TΓ2A predicts a too high critical temperature, $T^*\simeq 0.08$, which should be compared to the best estimate now available, $T^*=0.057$ [21]. The large disagreement is due to the fact that the TΓ2A is not a good theory for the RPM at low densities. In Fig. 5, coexistence densities—as obtained from the simulation results by Orkoulas and Panagiotopoulos [14]—have been included. Unfortunately, at low temperatures the vapor-liquid equilibrium of the RPM is still unknown. Because of that, we have estimated the orthobaric densities at low temperatures as the zero pressure densities calculated from the simulation data presented in Table VII. The low temperature orthobaric densities included in Fig. 5 have been calculated in this way. For the calculation of the triple point, it is convenient to have an analytical expression for the orthobaric densities. For $T^*<0.04$, the following relation is fulfilled:

$$\rho^*=1.1380-20.182T^*. \tag{4.3}$$

It should be mentioned that the expression proposed by Gillan [18] for describing orthobaric densities and used by other authors (see, for instance, Ref. [57]) seems inadequate in the light of the simulation data reported in this work. Apparently, the reason for the discrepancy is that Gillan used isochores in determining the zero pressure densities. This procedure can lead to densities lying beyond the mechanically stable fluid as two points of zero pressure may exist for a given isotherm at low temperatures.

For the computation of the fluid-solid equilibrium, in addition to the conditions in the equality of the pressures and chemical potentials of both phases, one has to assume a given structure for the solid phase. Two reasonable possibilities for the equilibrium solid at low temperatures are the CsCl and the NaCl structures. By using the theory of this work we were able to compute the fluid-solid (NaCl) transition at low temperatures. However, densities of the freezing for this transition were found to be larger than those for the fluid-solid (CsCl) coexistence. In other words, at the liquid densities at which the fluid-solid (NaCl) transition occurs the system would have already frozen into the CsCl structure. This result is in agreement with the conjecture of Stillinger and Lovett, [30] with the density functional theory of Barrat [31] as well as with the recent computer simulations of Smit *et al.* [32]. The reason that the NaCl structure does not appear seems to be clear. For the RPM, neither the internal energy (i.e., the Madelung constant) nor the free volume (the close packed density) favors the NaCl structure over the CsCl one.

The comparison of the simulation results with the theoretical calculations for the equilibrium liquid CsCl shows satisfactory agreement. The triple point evaluated through the cell and TΓ2A theories is located at $T_t^*=0.025$ to be compared with our estimate from the MC simulation, $T_t^*=0.0225$. For this, the tentative value $T^*=0.025$ has been recently reported by Smit *et al.* [32]. It has been obtained by extrapolating the high temperature fluid-solid (CsCl) equilibrium data calculated from their simulations. Regarding the coexistence densities, the curve on the fluid side obtained from our simulations is sharper than the theoretical one; thus, the theoretical triple point density is underestimated, $\rho_t^*=0.558$, while the pseudoexperimental value is $\rho_t^*=0.681$. It is interesting to relate the triple point temperature with that of the critical point. For the latter, we adopt here as the more confident estimate the value reported by Fisher and Levin, [21] $T_c^*=0.057$. The ratio T_t^*/T_c^* is 0.39 using the best estimates from simulation data for the RPM model. The ratio is close to the experimental one for ionic substances such as NaCl or CsCl, $T_t^*/T_c^*\approx 1/3$ [58]. Therefore the RPM provides an adequate basis to understand the low values of the triple point temperature to critical temperature ratio. Notice that this ratio is about 0.55 for nonionic systems such as noble gases.

There is another feature showing a different behavior of the RPM with respect to simple systems. It can be observed in Fig. 5 that the curve of coexistence densities in the solid (CsCl) phase is not monotonous. There is a change of slope at low temperatures resulting in a convex shape. In this

region, the solid densities increase as temperature decreases. Systems such as argon or nitrogen show a continuous decrease in the coexistence densities as the temperature decreases. This fact is predicted by the cell theory and confirmed by the computer simulation results of this work. This feature of the phase diagram of the RPM was not observed by Smit *et al.* since the temperature at which it appears is outside the range studied in their work. It is also absent in the phase diagram computed by Barrat [31] using a density functional theory. It would be interesting to know whether this feature is also present in the freezing of real molten salts such as NaCl and CsCl. A consequence of the negative slope of the solid coexistence curve is the large volume change at melting exhibited by the RPM model. At the triple point, the fractional density change, $(\rho^*_{\text{solid}}-\rho^*_{\text{liquid}})/\rho^*_{\text{solid}}$, is about 0.32. Figure 5 also shows the theoretical sublimation line estimated from the zero pressure densities of the CsCl solid. The solid densities along the sublimation line tend to the close packed density of the CsCl solid when the temperature goes to zero. This fact has also been observed in a quadrupolar hard-sphere fluid [43].

We have already mentioned that, at high temperatures, the fluid coexists with a solid arranged in the fcc structure. Indeed, it is clear that this must be the stable solid in the limit $\beta^*\to 0$. The appearance of the fcc structure at high temperatures can be understood on the basis that, under these conditions, Coulombic forces diminish their importance whereas the hard-sphere potential is not affected by the temperature. Thus the entropic term compensates the internal energy gain. This is correctly predicted by both theory and simulation (see Fig. 5). In Fig. 6, a more detailed view showing the fluid-solid (fcc) freezing line at very high temperatures is presented (it covers the range of temperatures just above those shown in the previous figure). There, it can be seen that the fluid-solid (fcc) freezing is almost a vertical line although it exhibits a very small slope. At $T^*=\infty$ our theoretical prediction for the coexistence densities of hard spheres is $\rho_f^*=0.933$ and $\rho_s^*=1.049$. These values are in very good agreement with the well stated simulation values, which are $\rho_f^*=0.943$ and $\rho_s^*=1.041$ [59,60]. Overall, the theory yields very good predictions for the coexistence densities along the fluid-solid (fcc) transition.

Let us return again to Fig. 5. The cell theory predicts the existence of a solid (CsCl)-solid (fcc) transition at low temperatures. This can be easily explained as the CsCl solid has a lower internal energy and a smaller close packing density than the fcc one. Since the solid stable structure at low temperatures is not the same as that at high temperatures, a second triple point must appear on the phase diagram. The coexisting phases are the fluid, a CsCl solid, and the fcc solid. Table X presents the coexisting properties obtained from the simulation data using the procedure described in Appendix II. Orthobaric densities for the liquid at low temperatures are also included. The precise location of this triple point in the usual $T^*-\rho^*$ plot is difficult as the lines of coexisting densities for solid phases are very steep. Figure 7 displays a P^*-T^* plot of the fluid-solid CsCl and fluid-solid fcc. It can be seen that the intersection of the curves allows a precise estimate of the ''simulated'' triple point, which occurs at $T^*=0.24$, $\rho^*=0.93$. Previous simulation results from Smit *et al.* [32] yielded for this triple point temperature

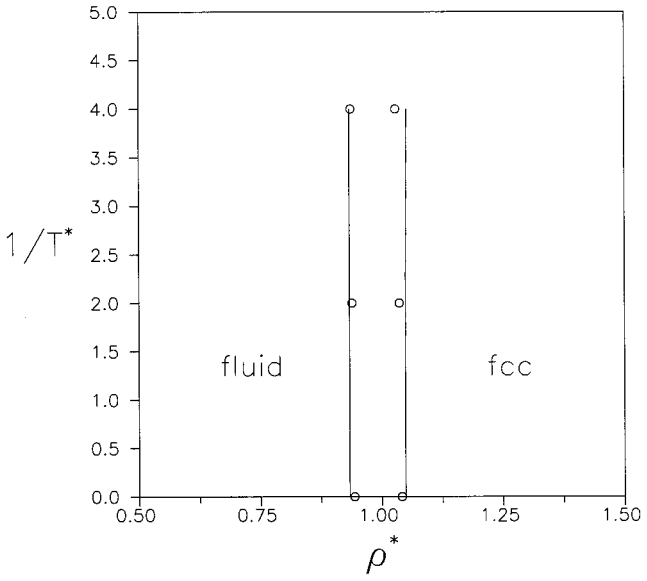

FIG. 6. Fluid-solid (fcc) equilibrium for the RPM model. Lines correspond to the theory of this work whereas the circles were obtained by using the computer simulations of this work except the value for hard spheres which is taken from Ref. [59].

$T^*\approx 0.30$. The cell theory locates it at $T^*=0.15$. The reason for the discrepancy is that the cell theory does not provide accurate values for the free energy of the CsCl solid at high temperatures (see Table IX). Even so, our estimate is much closer to the simulation results than that coming from the density functional theory by Barrat [31] who reported $T^*=0.045$. A more general comparison between the phase diagram as obtained from the theory of this work, from density functional theory and from the computer simulation of this work is given in Fig. 8. It is clear that the cell theory provides a much better description of the fluid-solid equilibrium than the Barrat theory [31]. A final remark about this region of the phase diagram is that the coexistence densities along the solid (CsCl)-solid (fcc) theoretical line tend to the close packed densities of each type of solid as the temperature goes to zero as can be expected.

The results presented in Fig. 5 show that the combination of the TΓ2A for the fluid phase with the cell theory for the solid phase yields a qualitatively correct phase diagram for the RPM. This is remarkable since all used expressions are quite simple to implement. Therefore, future applications on the solid-fluid equilibrium of charged systems should consider as a serious alternative the use of the cell theory for describing the solid phases.

V. CONCLUSIONS

In this work, the phase diagram of a charged hard-spheres model (RPM) was evaluated both theoretically and by using computer simulations. The emphasis is put on the fluid-solid equilibrium. We have shown how the cell theory of Lennard-Jones and Devonshire can be implemented for describing ionic solids. This theory provides a satisfactory description of the equation of state, internal energies, and free energies

TABLE X. Coexisting properties of the RPM as obtained from the simulation results of this work. The chemical potential is denoted as μ.

T^*	Phase 1	Phase 2	ρ_1^*	ρ_2^*	P^*	$\mu/(kT)$
0.5	fluid	fcc	0.939	1.036	5.64	14.07
0.25	fluid	fcc	0.936	1.026	2.72	12.42
0.25	fluid	CsCl	0.941	1.016	2.79	12.72
0.20	fluid	CsCl	0.911	0.991	1.91	10.34
0.15	fluid	CsCl	0.866	0.956	1.14	7.07
0.13	fluid	CsCl	0.844	0.936	0.87	5.31
0.04	fluid	CsCl	0.724	0.916	0.09	−12.95
0.025	fluid	CsCl	0.696	0.991	0.01	−26.57
0.03	gas	liquid		0.540	0	
0.0275	gas	liquid		0.582	0	
0.0225	gas	liquid		0.681	0	
0.0225	liquid	CsCl	0.681	1.000	0	

of the RPM system in the solid phase. When combined with an accurate treatment of the fluid phase, in particular the TΓ2A theory, a satisfactory description of the phase diagram is obtained. The predictions of the theory seem to be superior to the results obtained from the density functional theory of Barrat [31].

The computer simulations performed in this work provide the following picture for the phase diagram of charged hard spheres (it is to be mentioned that the phase diagram conjectured by Stillinger and Lovett almost 30 years ago seems to be qualitatively correct and adequate). At high temperatures the fluid is in equilibrium with a disordered fcc solid whereas at low temperatures freezing occurs into the CsCl structure, and then, two triple points have been found. Coexistence densities along the fluid-solid (fcc) equilibrium scarcely change with temperature. For the fluid-solid (CsCl) equilibrium, we found in the neighborhood of the triple point an increase of the solid density as the temperature decreases. In the first triple point, the fluid, a solid (CsCl), and a solid(fcc) are in equilibrium. In the second, the gas, the liquid and the solid CsCl are the coexisting phases. Our estimates of the triple point temperatures are $T^*=0.24$ for the former and $T^*=0.0225$ for the latter one. The ratio between the gas-liquid-solid (CsCl) triple point temperature and the critical one T_t^*/T_c^* is estimated as 0.39. This is in fair agreement with the value 1/3 found for a number of molten salts. The fractional density change at melting for the RPM is quite large. The final conclusion of this work is that by treating the solid with the very simple cell theory, an almost quantitative determination of the phase diagram can be obtained provided that it is combined with a good theory (such as the TΓ2A) for the liquid phase.

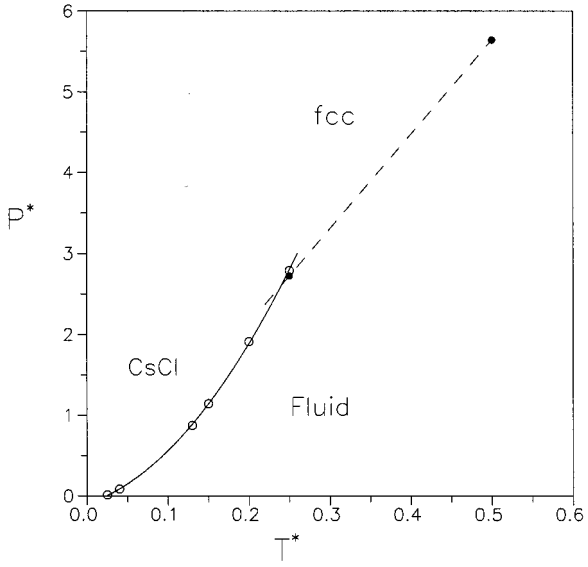

FIG. 7. P^*-T^* diagram obtained from the simulation results of this work (see Table X). Open circles correspond to the fluid-solid (CsCl) equilibrium, filled circles to the fluid-solid (fcc) coexistence. Lines are only a guide to the eye.

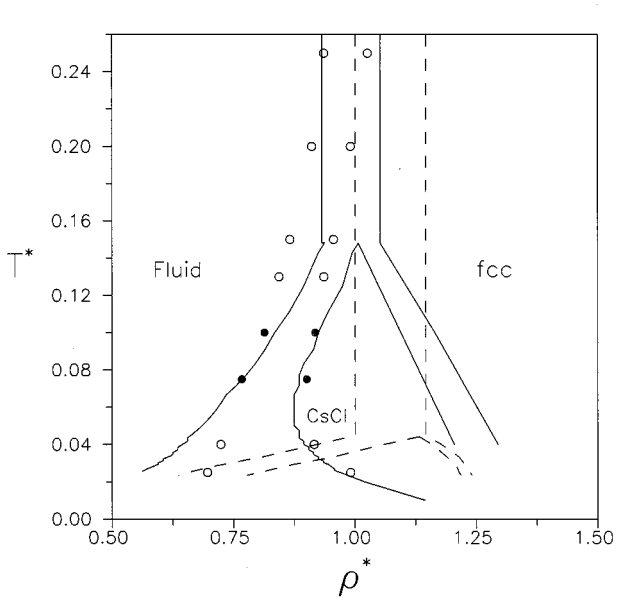

FIG. 8. A comparison between the fluid-solid equilibrium of the RPM model obtained from the cell theory (solid lines), from the density functional theory of Barrat [31] (dashed lines) and from computer simulation (symbols). Meaning of the symbols as in Fig. 5.

The phase diagram of the RPM model differs considerably from that of other models proposed for ionic systems such as the classical one component plasma (a system made of mobile ions immersed in a neutralizing background). The OCP fluid freezes into a body centered cubic lattice (bcc) *without changing its density* [24–26]. Somewhat related with the OCP is the Yukawa model. For this system freezing occurs into either a fcc or a bcc lattice depending on thermodynamic conditions, which seems similar to the behavior found in this work for the RPM. Nevertheless, there are at least two important differences. First, the fractional density changes at melting for the Yukawa models so far reported [27–29] are quite small in contrast with those of the RPM. Secondly, the bcc is quite different from the cesium chloride structure (the Bravais lattice of the latter is simple cubic [61]).

ACKNOWLEDGMENTS

This work has been partially supported by Projects No. PB94-0285 and PB93-0085 furnished by the Dirección General de Investigación Científica y Tecníca (DGICYT) of Spain.

APPENDIX A: TRUNCATED Γ2 APPROXIMATION

In this Appendix we give the expressions for the free energy, internal energy, and compressibility factor of the RPM model. They are given for completeness and we refer the interested reader to Ref. [3] for further details. Let us start defining two new magnitudes x and p (not to be confused with the pressure, which is denoted by P) as

$$x=(4\pi\rho^*\beta^*)^{1/2}, \tag{A1}$$

$$p=(1+2x)^{1/2}-1. \tag{A2}$$

The internal energy and the compressibility factor obtained from the MSA solution of the Ornstein-Zernike equation are given by

$$\frac{U^{\mathrm{MSA}}}{NkT}=-\frac{x^2+x-x(1+2x)^{1/2}}{4\pi\rho^*} \tag{A3}$$

and

$$Z^{\mathrm{MSA}}=Z^{\mathrm{HS}}+\frac{3x+2+3x(1+2x)^{1/2}-2(1+2x)^{3/2}}{12\pi\rho^*}, \tag{A4}$$

where Z^{HS} is the compressibility factor of hard spheres. For this, we use the Carnahan-Starling equation [62]

$$Z^{\mathrm{HS}}=\frac{1+y+y^2-y^3}{(1-y)^3}, \tag{A5}$$

being

$$y=\frac{\pi}{6}\rho^*. \tag{A6}$$

The expressions for the internal energy and compressibility factor of the TΓ2A are then given by

$$\frac{U^{\mathrm{T\Gamma 2A}}}{NkT}=\frac{U^{\mathrm{MSA}}}{NkT}-s\prime, \tag{A7}$$

and

$$Z^{\mathrm{T\Gamma 2A}}=Z^{\mathrm{MSA}}-s\prime, \tag{A8}$$

where the function $s\prime$ has been defined as

$$s'=\frac{p(p+2)}{512(p+1)}\{5p^2-6p+3+[4(2p-1)-\sin p-(4p-1)\cos p]e^{-p}\}. \tag{A9}$$

Finally, the TΓ2A free energy is given by

$$\frac{A^{\mathrm{T\Gamma 2A}}}{NkT}=\ln\frac{\rho^*}{2}-1+\frac{A^{\mathrm{HS}}}{NkT}-\frac{3x^2+6x+2-2(1+2x)^{3/2}}{12\pi\rho^*}-\frac{1}{128}\left\{\frac{5p^3}{3}-3p^2+3p+4-e^{-p}[4(2p+1)+(2p+1)\sin p-2p\cos p]\right\}, \tag{A10}$$

where $A^{\mathrm{HS}}/(NkT)$ is the residual Helmholtz free energy of hard spheres, which can be obtained by integrating the Carnahan-Starling equation so that

$$\frac{A^{\mathrm{HS}}}{NkT}=y\frac{4-3y}{(1-y)^2}. \tag{A11}$$

Equations (A1)–(A11) provide all that is needed for a full description of the fluid phase of the RPM.

APPENDIX B: DETERMINATION OF THE PHASE DIAGRAM FROM SIMULATION DATA

In this appendix we sketch the procedures necessary for obtaining the phase diagram and (especially) the interpolations used for the calculation of the triple points from the discrete simulation data.

(i) The fluid is parametrized through the TΓ2A theory along with the empirical corrections given by Eqs (4.1) and (4.2), which brings the theory in close agreement with the simulation results of this work. This empirical correction is used for densities in the range $0.55<\rho^*<0.75$. For larger densities, no correction term was used since the TΓ2A yields very good agreement with simulation.

(ii) Orthobaric densities of the liquid at low temperatures were approximated as the zero pressure densities using the MC data of Table VII. For $T^*<0.040$, the orthobaric densi-

ties may be described by Eq. (4.3).

(iii) The equation of state for the CsCl and fcc solids at several isotherms were obtained from the computer simulations of this work. At each temperature, the compressibility factor was fitted to a polynomial function on density.

(iv) The free energy of the CsCl solid at $T^*=0.05$ and $\rho^*=1$ was taken from the work of Smit *et al.* [32]. Free energies of the CsCl solid at other temperatures and densities were obtained by using thermodynamic integration and the simulation results of this work.

(v) The free energies of the fcc solid were obtained by using thermodynamic integration from the relation

$$\frac{A_{\rm fcc}^{\rm RPM}(\rho^*,\beta^*)}{NkT}=5.632-\ln 2+\int_0^{\beta^*}\frac{U(\rho^*=1.10,\beta'^*)}{NkT}\frac{d\beta'^*}{\beta'^*}+\int_{1.10}^{\rho^*}\frac{Z(\rho'^*,\beta^*)}{\rho'^*}d\rho'^*. \tag{B1}$$

The first two terms in Eq. (B.1) are the free energy of the RPM fcc solid for $\rho^*=1.10$ and $\beta^*=0$. This is obtained by using the well-known value of the hard-sphere free energy [59,60] for the fcc solid at $\rho^*=1.10$ (5.632 in NkT units) and the extra contribution due to the random mixing of cations and anions at $\beta^*=0$ (the $-\ln 2$ term).

[1] J.A. Barker and D. Henderson, Annu. Rev. Phys. Chem. **23**, 439 (1972).
[2] J.D. Weeks, D. Chandler, and H.C. Andersen, J. Chem. Phys. **54**, 5237 (1971).
[3] B. Hafskjold and G. Stell, *The Liquid State of Matter*, edited by E.W. Montroll and J.L. Lebowitz (North-Holland, Amsterdam, 1982).
[4] E. Waisman and J.L. Lebowitz, J. Chem. Phys. **56**, 3086 (1972).
[5] E. Waisman and J.L. Lebowitz, J. Chem. Phys. **56**, 3093 (1972).
[6] D.N. Card and J.P. Valleau, J. Chem. Phys. **52**, 6232 (1970).
[7] B. Larsen, J. Chem. Phys. **65**, 3431 (1976).
[8] J.C. Rasaiah, D.N. Card, and J.P. Valleau, J. Chem. Phys. **56**, 248 (1972).
[9] B. Larsen, G. Stell, and K.C. Wu, J. Chem. Phys. **67**, 530 (1977).
[10] B.P. Chasovskikh and P.N. Vorontsov-Vel'yaminov, High Temp. (USSR) **13**, 1071 (1975).
[11] P.N. Vorontsov-Vel'yaminov and B.P. Chasovskikh, High Temp. (USSR) **14**, 174 (1976).
[12] G. Stell, K.C. Wu, and B. Larsen, Phys. Rev. Lett. **37**, 1369 (1976).
[13] G. Orkoulas and A.Z. Panagiotopoulos, Fluid Phase Equilibria **93**, 223, (1993).
[14] G. Orkoulas and A.Z. Panagiotopoulos, J. Chem. Phys. **101**, 1452 (1994).
[15] J.M. Caillol, J. Chem. Phys. **100**, 2161 (1994).
[16] J.M. Caillol and J.J. Weis, J. Chem. Phys. **102,** 7610 (1995).
[17] J.C. Shelley and G.N. Patey, J. Chem. Phys. **103**, 8299 (1995).
[18] M.J. Gillan, Mol. Phys. **49**, 421 (1983).
[19] K.S. Pitzer and D.R. Schreiber, Mol. Phys. **60**, 1067 (1987).
[20] F. Bresme, E. Lomba, J.J. Weis, and J.L.F. Abascal, Phys. Rev. E **51**, 289 (1995).
[21] M.E. Fisher and Y. Levin, Phys. Rev. Lett. **71**, 3826 (1993).
[22] K.S. Pitzer, J. Phys. Chem. **99**, 13070 (1995).
[23] M.E. Fisher, J. Stat. Phys. **75**, 1 (1994).
[24] E.L. Pollock and J.P. Hansen, Phys. Rev. A **8**, 3110 (1973).
[25] G.S. Stringfellow, H.E. De Witt, and W.L. Slattery, Phys. Rev. A **41**, 1105 (1990).
[26] R.T. Farouki and S. Hamagouchi, Phys. Rev. E **47**, 4330 (1993).
[27] E.J. Meijer and D. Frenkel, J. Chem. Phys. **94**, 2269 (1991).
[28] G. Dupont, S. Moulinasse, J.P. Ryckaert, and M. Baus, Mol. Phys. **79**, 453 (1993).
[29] M.J. Stevens and M.O. Robbins, J. Chem. Phys. **98**, 2319 (1993).
[30] G.H. Stillinger and R. Lovett, J. Chem. Phys. **54**, 1086 (1968).
[31] J.L. Barrat, J. Phys. C **20**, 1031 (1987).
[32] B. Smit, K. Esselink, and D. Frenkel, Mol. Phys. **87**, 159 (1996).
[33] J.E. Lennard-Jones and A.F. Devonshire, Proc. R. Soc. London Ser. A **168**, 53 (1937).
[34] J.A. Barker, *Lattice Theories of the Liquid State* (MacMillan, New York, 1963).
[35] D. Henderson and J.A. Barker, Mol. Phys. **14**, 587 (1968).
[36] M. Baus, J. Phys. Condens. Matter **2**, 2111 (1990).
[37] A.D.J. Haymet, Annu. Rev. Phys. Chem. **38**, 89 (1987).
[38] J.D. McCoy, S. Singer, and D. Chandler, J. Chem. Phys. **87**, 4853 (1987).
[39] S.J. Smithline and A.D.J. Haymet, J. Chem. Phys. **86**, 6486 (1987).
[40] E.P.A. Paras, C. Vega, and P.A. Monson, Mol. Phys. **77**, 803 (1992).
[41] E.P.A. Paras, C. Vega, and P.A. Monson, Mol. Phys. **79**, 1063 (1993).
[42] C. Vega and P.A. Monson, Mol. Phys. **85**, 413 (1995).
[43] C. Vega and P.A. Monson, J. Chem. Phys. **102**, 1361 (1995).
[44] X. Cottin and P.A. Monson, J. Chem. Phys. **99**, 8914 (1993).
[45] X. Cottin and P.A. Monson, J. Chem. Phys. **102**, 3354 (1995).
[46] P.A. Monson, X. Cottin, E.P.A. Paras, and C. Vega, Fluid Phase Equilibria **117**, 114 (1996).
[47] T.L. Hill, *Statistical Mechanics* (McGraw-Hill, New York, 1956).
[48] D. Quane, J. Chem. Education **47**, 396 (1970).
[49] D.A. McQuarrie, J. Phys. Chem. **66**, 1508 (1962).
[50] J.R. Reitz and F.J. Milford, *Foundations of Electromagnetic Theory* (Addison-Wesley, Reading, 1966).
[51] R.J. Buehler, R.H. Wentorf, Jr., J.O. Hirschfelder, and C.F. Curtiss, J. Chem. Phys. **19**, 61 (1951).
[52] B.J. Alder, W.G. Hoover, and D.A. Young, J. Chem. Phys. **49**, 3688 (1968).
[53] R. Kubo, *Statistical Mechanics* (North-Holland, Amsterdam, 1965).
[54] M.P. Allen and D.J. Tildesley, *Computer Simulation of Liquids* (Clarendon Press, Oxford, UK, 1987).

[55] P.P. Ewald, Ann. Phys. (Leipzig) **64**, 253 (1921).
[56] L. Onsager, J. Phys. Chem. **43**, 189 (1939).
[57] K.S. Pitzer, Chem. Phys. Lett. **105**, 484 (1984).
[58] A.R. Ubbelohde, *The Molten State of Matter* (Wiley, Chichester, 1978).
[59] W.G. Hoover and F.H. Ree, J. Chem. Phys. **49**, 3609 (1968).
[60] D. Frenkel and A.J.C. Ladd, J. Chem. Phys. **81**, 3188 (1984).
[61] C. Kittel, *Introduction to Solid State Physics* (Wiley, New York, 1986).
[62] N.F. Carnahan and K.E. Starling, J. Chem. Phys. **51**, 635 (1969).